Soria-Verdugo, Antonio… et al. (2020) Comparison of wood pyrolysis kinetic data derived from thermogravimetric experiments by model-fitting and model-free methods, *Energy Conversion and Management*, v. 212, 112818, pp.: 1-12.

DOI: https://doi.org/10.1016/j.enconman.2020.112818

Comparison of wood pyrolysis kinetic data derived from thermogravimetric experiments by model-fitting and model-free methods

Antonio Soria-Verdugo[a]*, Marco Tomasi Morgano[b], Hartmut Mätzing[c], Elke Goos[d], Hans Leibold[c], Daniela Merz[c], Uwe Riedel[d], Dieter Stapf[c]

[a] *Carlos III University of Madrid (Spain), Energy Systems Engineering Group, Thermal and Fluids Engineering Department. Avda. de la Universidad 30, 28911 Leganés, Madrid (Spain).*

[b] *ARCUS Greencycling Technologies GmbH, Leonberger Straße 30, D-71638 Ludwigsburg (Germany).*

[c] *Karlsruhe Institute of Technology (KIT), Institute for Technical Chemistry (ITC), Hermann-von-Helmholtz-Platz 1, 76344 Eggenstein-Leopoldshafen (Germany).*

[d] *Deutsches Zentrum für Luft- und Raumfahrt e.V. (German Aerospace Center, DLR), Institute of Combustion Technology, Pfaffenwaldring 38-40, 70569 Stuttgart (Germany).*

* *corresponding author: asoria@ing.uc3m.es Tel: +34916248465.*

Abstract

The pyrolysis kinetics of beech wood was analyzed using model-free and model-fitting methods. Experimental measurements of the pyrolysis process were conducted in two thermogravimetric analyzers (TGA), a TG 209/2/F from Netzsch and a TGA Q500 from TA Instruments, which were found to have a similar precision in the establishment of the preset heating rate. Two experimental procedures were employed: (i) introducing samples which were pre-dried externally before the experiments were executed and (ii) internal (in situ) drying

of the samples in the TGA via a special temperature program below 150 °C which preceded the pyrolysis process.

The kinetic parameters were derived (i) using several model-free methods, namely Kissinger method, isoconversional methods, a simplified Distributed Activation Energy Model (sDAEM) and, (ii) using a model-fitting method via a five-step reaction model which calculates the differential thermogravimetric (DTG) curves at different heating rates; the calculated DTG curves were further analyzed by Kissinger's method to obtain overall kinetic data.

The kinetic parameters were found to be different in the two experimental procedures. Also, they turned out different when the assumed end temperature of the pyrolysis process was varied. This is because the pyrolysis of slowly charring solid residues becomes more important with increasing temperature and finally overruns the release of volatiles from the wood samples. For the same experimental procedure and for sufficiently low end temperatures, corresponding to a degree of conversion less than 85 %, model-free and model-fitting methods resulted in similar kinetic parameters.

Keywords**:** biomass pyrolysis; pyrolysis kinetics; model-free methods; model-fitting methods.

Nomenclature

A	pre-exponential factor of rate coefficient [s^{-1}]
α	degree of conversion [%]
β	heating rate [K min^{-1}, K s^{-1}]
β_{mea}	heating rate measured by the TGA [K min^{-1}, K s^{-1}]

47	β_{set}	heating rate programmed to the TGA [K min^{-1}, K s^{-1}]
48	E	activation energy [kJ mol^{-1}]
49	E_0	mean value of Gaussian distribution of activation energy [kJ mol^{-1}]
50	E_α	activation energy for a specific value of the conversion degree [kJ mol^{-1}]
51	ε	average relative error [%]
52	ε_A	average relative error of the pre-exponential factor A [%]
53	ε_E	average relative error of the activation energy E [%]
54	$f(\alpha)$	differential form of the α-dependent part of the rate equation [-]
55	$g(\alpha)$	integral form of the α-dependent part of the rate equation [-]
56	$h(E)$	probability density function of the activation energy [mol kJ^{-1}]
57	k	rate coefficient/constant of a first-order reaction [s^{-1}]
58	m	mass of the sample remaining [g]
59	m_0	initial mass of the sample at the beginning of TGA test [g]
60	m_{pi}	mass of the sample remaining at the beginning of the pyrolysis [g]
61	m_{pf}	mass of the sample remaining once the pyrolysis is completed [g]
62	n	order of the pyrolysis reaction [-]
63	N	total number of heating rates considered [-]
64	$\nu_{i,j}$	stoichiometric coefficient of carbon from component *i* in reaction *j* [-]
65	R	universal gas constant [J mol^{-1} K^{-1}]
66	R^2	determination coefficient [-]
67	t	time [min]
68	T	temperature [ºC, K]
69	T_0	initial temperature of the pyrolysis process [ºC, K]
70	T_{max}	temperature at which the reaction rate has its maximum [ºC, K]
71	X	percentage of mass of the sample remaining [%]

X_{pi} percentage of mass remaining at the beginning of pyrolysis process [%]

X_{pf} percentage of mass remaining at the end of pyrolysis process [%]

Abbreviations:

CFD	Computational Fluid Dynamics
DTG	Differential Thermogravimetric
HHV	Higher Heating Value
KAS	Kissinger-Akahira-Sunose
LHV	Lower Heating Value
OFW	Ozawa-Flynn-Wall
sDAEM	simplified Distributed Activation Energy Model
TG	Thermogravimetric
TGA	Thermogravimetric Analysis / Thermogravimetric Analyzer

1. Introduction

Biomass is one of the most widely used renewable energy carriers due to its worldwide availability, its net carbon dioxide neutral character, and because it is easy to store, which permits decentralized production of heat and power on-demand. Furthermore, the local availability of biomass can increase fuel security and reduce carbon dioxide emissions associated with fuel transportation [1]. Biomass can be transformed via biochemical, physico-chemical, and thermochemical processes [2]. This paper is on pyrolysis, defined as thermal degradation in the absence of oxygen and other gasifying media [3]. Pyrolysis presents several benefits, such as the use of moderate temperatures (300-600 ºC), the mostly small amount of pollutant emissions, and the possibility to obtain a high-quality liquid fuel, easy to handle, store and transport.

Pyrolysis of biomass can be studied using thermogravimetric analysis (TGA) or differential scanning calorimetry (DSC) [4]. The goal of TGA is to determine the global kinetic parameters of biomass pyrolysis processes (activation energies and pre-exponential factors), which in combination with other analytical measurement techniques helps to clarify the thermal decomposition process and to understand the product formation from the pyrolysis reactions. Moreover, these global kinetic data can also be employed for the design and optimization of pyrolysis reactors and as input parameters for CFD simulations [5].

The derivation of the kinetic parameters can be based on model-fitting or on model-free methods. Model-fitting methods require an assumption about the reaction mechanism and a suitable fit of the rate constants to match the overall results obtained from TGA measurements. In contrast, model-free methods assign only overall kinetic parameters to the decomposition process of the bulk sample. No effort is made in this case to clarify the product formation. Therefore, the computational procedure is relatively simple and the cost of model-free methods is low compared to the cost of model-fitting methods [6]. Vyazovkin et al. [7] consider that the kinetic parameters obtained from model-free methods are more consistent and reliable due to the absence of multiple assumptions made in model-based analyses. However, model-free methods yield less detailed information than model-fitting methods.

In previous studies of model-free methods, the fitting precision and the reliability of kinetic parameters were found to be directly related to the experimental uncertainty, which can be high [8,9]. In contrast, high fitting precision was demonstrated to be realized using model-free methods [10]. This emphasizes the

120 need for a critical comparison of the results obtained from model-free and model-
121 fitting kinetic methods, which is the major objective of the present study.

122 In this work, the pyrolysis of beech wood was studied experimentally by non-
123 isothermal thermogravimetric measurements performed in two different TGA
124 instruments. The main novelty of the work relies on analyzing the experimental
125 measurements conducted by two different research groups using two different
126 TGA apparatus, by means of several model-free and a model-fitting method.
127 Regarding model-free methods, various isoconversional models as well as the
128 simplified Distributed Activation Energy Model (sDAEM), which is a multi-step
129 method, were employed. In addition, a model-fitting method based on a five-step
130 mechanism was used. Another innovation of this work is the use of different
131 drying procedures for the beech wood samples. The different drying procedures
132 tested were found to yield different pyrolysis kinetic data. Furthermore, the kinetic
133 parameters were determined selecting different final temperatures for the
134 pyrolysis process. In this way, the effect of the increasing contribution of
135 secondary char pyrolysis to the whole pyrolysis process could be quantified.

136 **2. Theory**

137 Model-free methods permit the computation of the kinetic parameters for specific
138 values of the pyrolysis conversion degree, requiring no assumptions about the
139 reaction mechanism. Most of them describe biomass pyrolysis kinetics by an
140 assumed single-step overall rate equation:

141 $$\frac{d\alpha}{dt} = k(T) f(\alpha), \quad (1)$$

142 employing the degree of conversion α, which is a dimensionless quantity, rather
143 than the measured sample mass *m*. The rate of reaction dα/d*t* is expressed as a
144 function of temperature *k(T)* and a function of the conversion *f*(α), which depends
145 on the reaction order.

146 For consistency, the International System of units (kg, m, s, K) is used for all the
147 variables included in the equations presented in this work.

148 For the rate coefficient, the most widely used temperature dependence
149 expression is that proposed by Arrhenius [11]:

150 $$k(T) = A\exp\left(-\frac{E}{RT}\right), \quad (2)$$

151 where *A* is the pre-exponential factor, *E* is the activation energy, *R* is the universal
152 gas constant, and *T* is the temperature. The resulting kinetic parameters may be
153 dependent on the degree of conversion. Also, they may be understood to
154 represent some average of all microscopic processes which contribute to the total
155 pyrolysis process. Model-free methods include Kissinger's method,
156 isoconversional methods, and multi-step methods, like the simplified Distributed
157 Activation Energy Model (sDAEM), which are described in detail below. The
158 Kinetics Committee of the International Confederation for Thermal Analysis and
159 Calorimetry (ICTAC) recommends the calculation of kinetic parameters from
160 isoconversional models for a wide range of conversion values, from 5% to 95%
161 [7]. In addition, the sDAEM has been widely used to derive pyrolysis kinetic data.

162 Model-fitting methods interpret and approximate the measured mass loss (i) by
163 generalized reaction mechanisms, templates of which are available in the

literature [12-14] or (ii) by individually developed reaction mechanisms, which usually involve a set of several first order reactions.

The template reaction mechanisms (i) represent decomposition processes which are relevant to any type of solids, not only solids of biogenic origin. Hence, they focus on n-th order reaction mechanisms, on the evolution of lattice defects in crystals, on diffusion limited decompositions, etc. In contrast, individually developed reaction mechanisms (ii) involve explicit reaction schemes which were developed for the specific substance under investigation, like the famous Broido-Shafizadeh models for the pyrolysis of cellulose [15,16] and numerous modifications and refinements thereof, as reviewed by Antal et al. [17] and by Conesa et al. [18]. Of course, the published reaction mechanisms vary considerably in the detailed description of various decomposition pathways, some of them [19] even consider thermodynamic data of the involved substances and specific processes at the molecular level, as reviewed recently by Wang et al. [6]. In practice, a good compromise is sought between user friendly applicability, completeness and accuracy.

It is emphasized here that the rate constants of such explicit mechanisms are not generally valid, because they do not refer to elementary reactions, but to composite reactions of biopolymers. Therefore, none of the reported rate constants is applicable to a different reaction scheme. They are valid only within the frame of the particular reaction mechanism for which they were developed. Other limitations of global mechanisms are the neglect of reverse reaction pathways and of heat release or consumption, but this is beyond the scope of this paper.

As noticed repeatedly in the literature, the kinetic data (*A*, *E*) derived from model-fitting or from model-free approaches vary substantially; famous examples are the round robin studies of the thermal decomposition of cellulose [20] and calcium carbonate [21]. Besides systematic errors, the data handling and the methods of data evaluation came into focus and were shown to contribute to the scattering of kinetic results [21-23].

2.1. Kissinger method

The Kissinger method [24,25] is based on the differential form of the rate equation. It relates the temperature T_{max}, at which the rate of reaction, $d\alpha/dt$, reaches a maximum, to the heating rate β. In case of a first order reaction, the relation reads:

$$\ln\left(\frac{\beta}{T_{\max}^2}\right) = \ln\left(\frac{AR}{E}\right) - \frac{E}{RT_{\max}}. \quad (3)$$

This characteristic equation can be employed to determine the pre-exponential factor *A* and the activation energy *E* of the pyrolysis reactions from a set of differential thermogravimetric (DTG) curves obtained at different heating rates β. Eq. (3) is exact only for single and pure substances which decompose according to a first-order reaction. However, for complex solid fuels such as biomass, Kissinger's method produces single values of *A* and *E* averaged over all individual physico-chemical processes, which in reality vary with the degree of conversion α. Therefore, the results obtained from the Kissinger method should be considered carefully. It is recommended to cross-check the dependence or independence of the kinetic parameters on the degree of conversion by an isoconversional method or by sDAEM [26].

2.2. Isoconversional methods

The isoconversional methods can be classified into differential and integral methods, depending on the form of the rate equation on which they are based [6]. The only differential isoconversional method of practical importance is the Friedman method [27], whereas a variety of integral isoconversional methods are in common use, e.g., the Ozawa-Flynn-Wall (OFW) method [28,29] and the Kissinger-Akahira-Sunose (KAS) method [24,30].

The characteristic equation of the Friedman model, Eq. (4), is obtained directly from the logarithm to the differential form of the rate equation, Eq. (1). For the assumed first order kinetics of the pyrolysis process, $f(\alpha) = 1 - \alpha$ [31], hence:

$$\ln\left(\frac{d\alpha}{dt}\right) = \ln\left(A\left(1-\alpha\right)\right) - \frac{E}{RT}. \tag{4}$$

The integral isoconversional methods make use of the integral form of the rate equation:

$$g\left(\alpha\right) = \int_0^{\alpha} \frac{d\alpha}{f\left(\alpha\right)} = \frac{A}{\beta}\int_{T_0}^{T} \exp\left(-\frac{E}{RT}\right)dT \approx \frac{A}{\beta}\int_0^{T} \exp\left(-\frac{E}{RT}\right)dT. \tag{5}$$

This integral employs the isoconversional principle according to which A and E are independent of temperature. The lower integration limit T_0 can be approximated by 0, since usually the degree of conversion below the starting temperature is negligible [28]. The integral in Eq. (5) is the so-called temperature integral, $I(E,T)$. It has no analytical solution, thus, Eq. (5) needs to be solved by approximation or by numerical integration [26].

231 The OFW [28,29] method uses the approximation of Doyle in Eq. (5) [32]. For first
232 order reactions, the function *g* is $g(\alpha) = -ln(1-\alpha)$ [31], and the OFW characteristic
233 equation yields:

234 $$\ln\beta = \ln\left(-\frac{AE}{R\ \ln(1-\alpha)}\right) - 5.3305 - 1.052\frac{E}{RT}. \quad (6)$$

235 The Kissinger-Akahira-Sunose (KAS) method [24,30] improves the accuracy of
236 the OFW method by using the approximation of Murray and White [33] for the
237 temperature integral instead of Doyle's approximation. The characteristic
238 equation then reads:

239 $$\ln\left(\frac{\beta}{T^2}\right) = \ln\left(-\frac{AR}{E\ \ln(1-\alpha)}\right) - \frac{E}{RT}. \quad (7)$$

240 Further details of the mathematical derivation of the isoconversional kinetic
241 methods can be found elsewhere [10, 34]. Corresponding to the validity of the
242 approximations to the temperature integrals, the expected numerical accuracy of
243 KAS method is higher than that of OFW method.

244 2.3. Simplified Distributed Activation Energy Model (sDAEM)

245 The Distributed Activation Energy Model (DAEM) proposed by Vand [35]
246 assumes the pyrolysis of a solid fuel to be a superposition of a large number of
247 independent first-order Arrhenius type reactions with different activation energies,
248 which can be represented by a continuous probability density function *h(E)*, with
249 units of inverse activation energy. For a constant heating rate β = d*T*/d*t*, the
250 degree of conversion α for the original DAEM can be written:

$$\alpha = 1 - \int_0^{\infty} \exp\left[-\frac{A}{\beta} \int_0^T \mathrm{e}^{-E/RT} \mathrm{d}T \right] h(E) \mathrm{d}E. \quad (8)$$

The exponential function in Eq. (8) is the so-called ϕ function. For the original DAEM, the form of the probability density function of the activation energy should be assumed to follow any statistical distribution like Gaussian, Weibull, etc. Thus, the original DAEM is an implicit model-fitting kinetic method.

Miura [36] and Miura and Maki [37] proposed a simplified DAEM (sDAEM), which is an integral model-free multi-step method. In view of the rapid variation of the ϕ function from 0 to 1, Miura [36] proposed to approximate it by a step function for any specific value of the activation energy. Using the approximation of Coats and Redfern [38] for the temperature integral and the approximate value of 0.58 for the step variation, the ϕ function becomes:

$$\phi(E,T) = \exp\left[-\frac{A}{\beta} \int_0^T \mathrm{e}^{-E/RT} \mathrm{d}T \right] \approx \exp\left[-\frac{ART^2}{\beta E} \mathrm{e}^{-E/RT} \right] = 0.58. \quad (9)$$

Then, taking logarithms to Eq. (9), the characteristic equation for the sDAEM is:

$$\ln\left(\frac{\beta}{T^2} \right) = \ln\left(\frac{AR}{E} \right) + 0.6075 - \frac{E}{RT}. \quad (10)$$

Therein, *A* and *E* usually vary with α. Miura and Maki [37] proposed the use of several TG curves, measured at several constant heating rates β, to determine *A* and *E* for each value of α. Soria-Verdugo et al. [39,40] found that at least five TG curves should be used in order to reproduce the measured TG curves with reasonable accuracy. Moreover, characteristic sDAEM equations for time dependent heating rates are available now [40,41]. Overall, the numerical

accuracy of the sDAEM method is estimated to be comparable to the KAS method.

2.4. Model-fitting kinetic method

Originally, a three-step mechanism was developed for the independent decomposition of the three pseudocomponents, i.e., hemicellulose, cellulose, and lignin. Despite its plausibility, such an approach has limitations, because no particular consideration of the polymeric nature of the biomass is made, effects of inorganic constituents are neglected, etc. [43]. Moreover, such a model predicts the separation of the hemicellulose and cellulose peaks at low heating rates [44,45], which is contrary to experimental evidence [46]. This can be avoided by increasing the number of reactions. The five-step model includes two parallel decomposition pathways for cellulose, one of which leads to intermediate tar formation. As default tar species levoglucosan was chosen, because it is a key species of wood pyrolysis and since the overall tar composition can be approximated by $C_6H_{10}O_5$, which is the sum formula of both the cellulose monomer and levoglucosan [46-49]. The five-step model is listed in Table 1.

Table 1: Reaction scheme of the five-step model [45,50].

compound	**reaction**[1)]	**A** [s^{-1}]	**E** [kJ/mol]
cellulose	$C_6H_{10}O_5 \rightarrow$ gas + 2.5 C	$2 \cdot 10^8$	132
cellulose	$C_6H_{10}O_5 \rightarrow$ 0.75 tar + gas + 0.625 C	$3 \cdot 10^{13}$	195
hemicellulose	$C_5H_8O_4 \rightarrow$ gas + 2 C	$1 \cdot 10^7$	105
lignin	$C_{10}H_{10}O_4 \rightarrow$ gas + 4.3 C	$1.5 \cdot 10^{14}$	192
tar	$C_6H_{10}O_5 \rightarrow$ gas	$2 \cdot 10^7$	122

[1)] gas composition is not a subject in this work; therefore, it is not specified here

The pseudocomponents are represented by their monomeric formulas and “gas” is a mixture of carbon monoxide (CO), carbon dioxide (CO_2), methane (CH_4),

hydrogen (H_2) and water vapor (H_2O) to complete the stoichiometry. Within this model, methane is a lump species which stands for all the non-tar hydrocarbons [50]. The kinetic data were obtained by manual fits to experimental DTG curves of several beech wood samples. The quality of such data fits is usually assessed by comparison to a model-free approach. Recently, the five-step model was extended to include dual decomposition reactions for all pseudo-components and two different tar species [51].

The kinetic parameters derived from these kinetic methods, either model-free or model-fitting, could be used in combination to heat and mass transfer models to simulate the pyrolysis process of wood in a bench scale or even industrial unit. The validity of the kinetic results derived from these methods for a bench scale facility was already demonstrated by Tomasi Morgano [52], however, the validity for industrial units should be evaluated.

3. Materials and methods

3.1. Feedstock analysis

European beech wood, *Fagus sylvatica*, was adopted for this study. Bark-free grinded material, particle size of 0.5-1.0 mm, was purchased from J. Rettenmaier und Söhne GmbH & Co. in Rosenberg, Germany. The feedstock was selected due to the extensive data available in the literature as well as for its high reproducibility and constant chemical composition.

Analysis of the feedstock was carried out following the respective German DIN Standards [53]. The chemical composition was determined by the Klason and Kürschner standards [54] to evaluate the content of cellulose, hemicellulose and

lignin. The results of the analysis are reported in Table 2. Considering the characteristics of beech wood reported in Table 2, the results of the kinetics analysis performed in this work are specific for wood. The results may differ for different solid samples such as polymers, coal, or non-lignocellulosic biomass.

Table 2: Characterization of the feedstock European beech wood (*Fagus sylvatica)*.

Parameter	Method	Value	Unit
Moisture	DIN EN 14774-2	9.7	wt.% ar
Proximate analysis			
Ash (550°C)	DIN EN 14775	1.4	wt.% db
Volatile matter	DIN EN 15148	83.3	wt.% db
Fixed carbon	analog to DIN 51734	15.3	wt.% db
Elemental analysis			
Carbon	DIN EN 15104	49.5	wt.% db
Hydrogen	DIN EN 15104	6.0	wt.% db
Nitrogen	DIN EN 15104	0.19	wt.% db
Oxygen*	DIN EN 15296	42.9	wt.% db
Trace elements			
Sulfur	DIN EN 15289	0.016	wt.% db
Chlorine	DIN EN 15289	< 0.005	wt.% db
Fluorine	analog to DIN EN 15289	< 0.001	wt.% db
Calorific values			
HHV	DIN EN 14918	19530	kJ/kg db
LHV	DIN EN 14918	18230	kJ/kg db
Chemical analysis			
Cellulose	Kürschner	44.9	wt.% daf
Hemicellulose	Sodium Chlorite $NaClO_2$[#]	33.9	wt.% daf
Lignin	Klason	21.2	wt.% daf

ar is as received; db is dry basis; daf is dry ash-free basis

* calculated by difference

[#] calculated from holocelullose

3.2. Thermogravimetric analyzers

Two different thermogravimetric analyzers (TGA) were employed to conduct pyrolysis tests: a TGA Q500 from TA Instruments located at BIOLAB in University

Carlos III of Madrid (UC3M), Spain and a TG 209/2/F from Netzsch located at the Institute for Technical Chemistry in Karlsruhe Institute of Technology (KIT), Germany. The technical specifications of both TGA instruments are included in Table 3, where the similarity of both devices can be seen.

Table 3: Technical specifications of TGA Q500 and TG 209/2/F.

Parameter	**TGA Q500**	**TG 209/2/F**
Maximum sample mass [g]	1	1
Mass measurement precision [%]	± 0.01	± 0.01
Mass resolution [μg]	0.1	0.1
Pan volume [μl]	100	85
Pan material	Platinum	Aluminum oxide
Furnace nitrogen flow rate [ml/min]	60	15
Balance nitrogen flow rate [ml/min]	40	10
Heating rate range [ºC/min]	0.01 – 100	0.1 – 80

The monitored variables during the pyrolysis tests in both TGA apparatus, i.e., time t, temperature T, percentage of mass remaining X, and variation of the percentage of mass remaining dX/dt, were recorded in temperature intervals of 0.1 ºC.

3.3. Pyrolysis measurements in TGA

The recommendations of the ICTAC kinetics committee [55] were considered for collecting the experimental thermal analysis data used for the kinetic computations. The initial sample mass was 10.5±0.5 mg. This mass is low enough to guarantee a negligible effect of heat and mass transfer inside the sample, while providing a high signal-to-noise ratio during the measurements.

The pyrolysis process was studied in two different procedures:

(i) external drying (experiments with pre-dried samples)

342 In these experiments, the wood samples were dried in a heated oven at 105 °C
343 for 24 hours to obtain a residual moisture close to 5 % and were protected against
344 ambient atmosphere until usage. During pyrolysis, the temperature was
345 increased from room temperature to 900 ºC at constant heating rates of 5, 10,
346 15, 25, 35, and 50 ºC/min. All experiments were repeated twice both in the TGA
347 Q500 and in the TG 209/2/F. The heating rates are low in comparison to industrial
348 applications; however, the kinetic parameters were previously found to be
349 independent of the heating rate in the range 20 – 200 ºC/min for some biomass
350 samples [56,57].

351 (ii) internal drying (in situ drying of the samples)

352 In these experiments, the samples were introduced into the TGA as received, i.e.,
353 containing approximately 10 wt.% of humidity, and a two-stage heating pyrolysis
354 was used in the TGA tests [58]. The temperature was first increased to 105 °C
355 and kept at that level for roughly 30 min, before starting the pyrolysis and heating
356 up further to 900 °C. The same six different values of the heating rate as for the
357 external drying tests were used for the in situ drying tests. The pyrolysis of the in
358 situ drying samples was conducted only in the TGA Q500 to quantify the effect of
359 the in situ process by comparison with the results of the pre-dried samples.

360 3.4. Processing of the TGA data

361 As already mentioned, the five-step model [45] was developed by manually fitting
362 the experimental DTG results of several beech wood pyrolysis experiments to the
363 set of five first order reactions, Table 1. For this purpose, the initial composition
364 of beech wood was set to 45 wt.% cellulose, 34 wt.% hemicellulose and 21 wt.%
365 lignin (daf, see Table 2). The total initial mass, the starting temperature T_0 and

366 the heating rate β were set to the experimental conditions. The time derivative of
367 the mass of each pseudocomponent *i* in reaction *j* was set to:

368 $$\frac{\mathrm{d}m_{i,j}}{\mathrm{d}t} = -A_{i,j} m_{i,j} \exp\left(-\frac{E_j}{RT}\right), \tag{11}$$

369 where the evolution of temperature *T* with time *t* is linear $T = T_0 + \beta \cdot t$. Note that,
370 of course, since cellulose has two decomposition pathways in the five-step model,
371 the time derivative of its mass is the sum of two rate expressions (*j* = 1 and 2).
372 Similarly, the time derivative of carbon (char) formation is:

373 $$\frac{\mathrm{d}m_C}{\mathrm{d}t} = \sum_j \sum_i A_{i,j} \nu_{i,j} m_{i,j} \exp\left(-\frac{E_j}{RT}\right), \tag{12}$$

374 where $\nu_{i,j}$ is the stoichiometric coefficient of carbon from component *i* in reaction
375 *j*. The differential equations were solved to obtain, amongst others, the total solid
376 mass (TG curve) and its time derivative (DTG curve) as a function of time and
377 temperature using a double precision version of the LSODE package from
378 Lawrence Livermore National Laboratory (LLNL) [59]. The numerical values for
379 $\nu_{i,j}$, $A_{j,j}$ and E_j are listed in Table 1 in section 2.4.

380 All model-free methods are based on the degree of conversion α and its rate of
381 variation $\mathrm{d}\alpha/\mathrm{d}t$ which were determined from the monitored variables of both TGA
382 apparatus. The degree of conversion α varies between 0 % at the beginning of
383 the pyrolysis process and 100 % when the pyrolysis is completed. The degree of
384 conversion α can be calculated as:

385 $$\alpha = 100 \cdot \frac{m_{pi} - m}{m_{pi} - m_{pf}}, \tag{13}$$

where m is the mass of the sample remaining at time t and m_{pi} is the initial mass of the sample when pyrolysis starts, i.e., at 150 ºC, and m_{pf} is the final mass of the sample once the reaction is completed. Its value varies a little depending on the temperature which is chosen to be the final temperature of the pyrolysis process. Then, dividing by the initial mass of the sample employed in the TGA test m_0, the degree of conversion α can be expressed in terms of the current mass percentage which is the output reading of the instruments:

$$\alpha = 100 \cdot \frac{X_{pi} - X}{X_{pi} - X_{pf}}. \tag{14}$$

In view of the definition of the degree of conversion α as a function of the percentage of mass remaining X, Eq. (14), the rate of variation of α can be related to the rate of variation of X as:

$$\frac{\mathrm{d}\alpha}{\mathrm{d}t} = -\frac{1}{X_{pi} - X_{pf}} \frac{\mathrm{d}X}{\mathrm{d}t}. \tag{15}$$

4. Results and discussion

4.1. Precision of heating rates in the two TGA instruments

In a TGA, the desired change of the sample temperature with time is pre-set by the programmed heating rate. However, the real sample temperature lags behind the programmed temperature and behind the temperature reading. The exact discrepancy is due to several instrument properties and operation conditions like location of the thermocouple, nature and flow rate of the inert carrier gas, heating rate, sample mass and particle size distribution, as well as the reaction heat. The thermal lag error increases at faster scanning rates, larger sample masses,

407 higher weight sample pans, etc. Therefore, the capability of the TGA to maintain
408 the heating rate at a constant value β_{set} during the whole process is a
409 characteristic of the instrument with the pan system, the employed experimental
410 conditions and the sample itself. To compare the instruments' performance
411 considering their specifications and the given different operation conditions
412 (Table 3 without considering the maximum sample mass) the heating rates
413 obtained in both TGAs during all the beech wood pyrolysis tests were determined
414 in a post-processing procedure as the time derivative of the temperature output
415 reading. This parameter is denoted β_{mea}. A moving average filter of 250 points
416 was used for the calculation of β_{mea} to avoid the numerical noise produced by the
417 derivation. The comparison of both TGA instruments in terms of their capability
418 to maintain the heating rate at β_{set} was carried out based on the relative error of
419 the heating rate:

420 $$\varepsilon_{\beta} = \frac{\beta_{set} - \beta_{mea}}{\beta_{set}}. \quad (16)$$

421 The values of ε_{β} are plotted in Figure 1 as a function of temperature for all the
422 pyrolysis experiments conducted in both TGA instruments. In both cases, the
423 accuracy of the equipment to maintain a set value for the heating rate is higher
424 for low heating rates and for high temperatures, as a consequence of the time
425 required by the instruments to adjust to the programmed value of β. However, the
426 behavior of both TGAs differs, especially for high values of the heating rate. The
427 TGA Q500 approaches the selected value of β from slightly lower values,
428 whereas the TG 209/2/F seems to overshoot the set value of β and approximate
429 to it from higher values. This results in positive values for the relative error of the

heating rate, Eq. (16), for the TGA Q500, whereas negative values of ε_β were obtained for the TG 209/2/F. In terms of the deviation from the selected value of the heating rate, the TGA Q500 is very accurate for the whole range of temperatures analyzed for values of β below 25 ºC/min. In contrast, deviations similar to those obtained in the TGA Q500 for heating rates of 35 ºC/min occur in the TG 209/2/F for values of 15 ºC/min. In addition, the maximum variations for heating rates up to 50 ºC/min in the temperature range of 150 – 600 ºC is 8.5 % for the TG 209/2/F and 4 % for the TGA Q500. Nevertheless, for temperatures above 300 ºC, where most of the pyrolysis of lignocellulosic biomass occurs, the deviations of the heating rate are within 1.5 % for the TGA Q500 and 5 % for the TG 209/2/F, which are acceptable values in both cases.

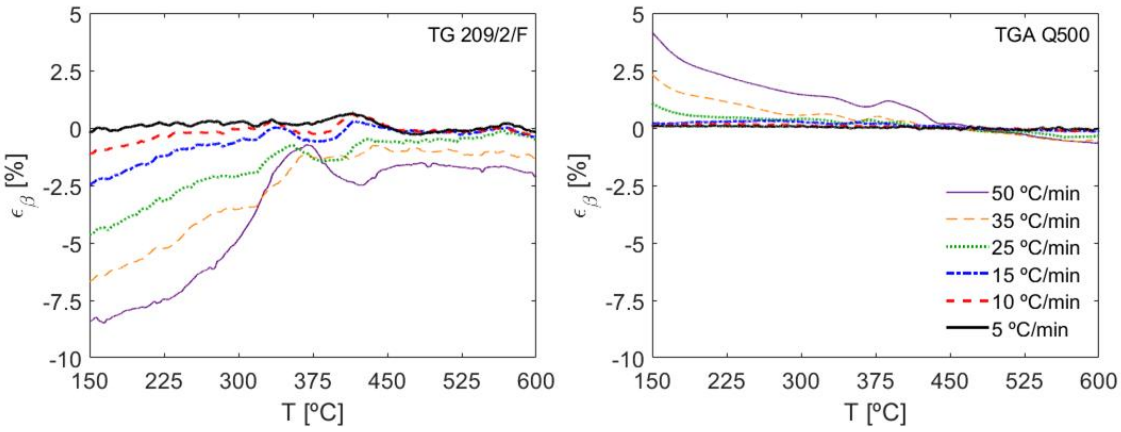

Figure 1: Relative error of the heating rate for all the pyrolysis tests in both TGA instruments during the pyrolysis of the pre-dried samples.

4.2. TG and DTG curves obtained for the pre-dried samples in both TGAs

The measured TG and DTG curves for the pre-dried beech wood samples are plotted in Figure 2 for both instruments.

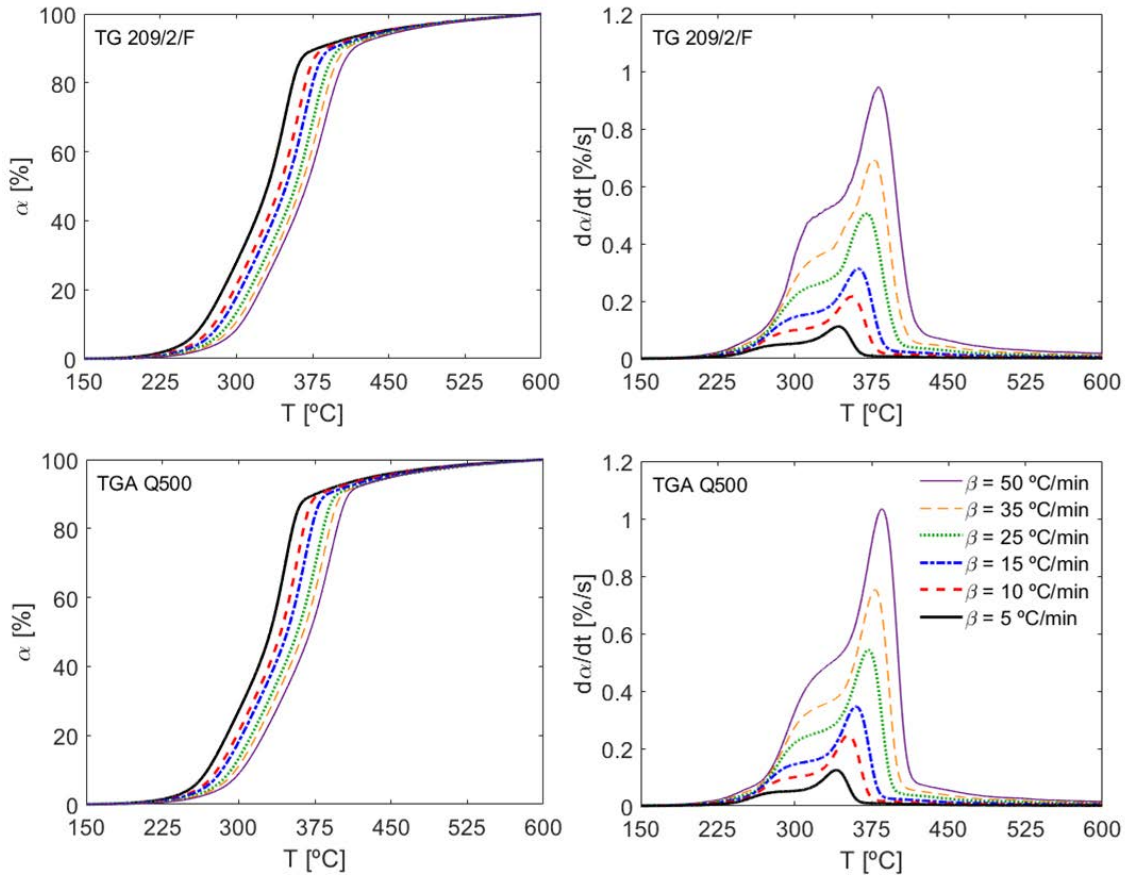

Figure 2: TG and DTG curves for the pyrolysis of beech wood at various heating rates in both TGA instruments (pre-dried samples).

The TG curves show a steep increase of the degree of conversion in a temperature range between approximately 250-400 ºC, followed by a smooth increase of the degree of conversion towards higher temperatures, for all the heating rates tested. In this temperature range, most of the volatile matter contained in lignocellulosic biomass is released and decomposed, followed by the subsequent slow pyrolysis of the char produced. As a consequence of the non-isothermal experimental procedure, an increase of the heating rate β induces a shift of the decomposition process to higher temperatures, in agreement with literature data [25,60,61].

459 The structure of the DTG curves has often been interpreted to originate from
460 overlapping peaks in the literature. In this sense, two overlapping peaks can be
461 observed at temperatures between 250 and 400 ºC. These may be attributed to
462 the pyrolysis of the hemicellulose and cellulose. A third underlying peak, which
463 covers a wide range of temperatures between 200 ºC and 500 ºC, cannot be
464 observed directly, but is expected to represent the comparatively slow pyrolysis
465 of lignin [47].

466 For the pre-dried samples, the agreement between the experimental results
467 obtained in the two thermogravimetric analyzer TG 209/2/F and TGA Q500 was
468 good with relative errors around 2 % in α for TG and 10 % in dα/dt for DTG data.
469 The differences are probably due to small differences of the thermal lags.

470 4.3. Results of model-free methods

471 4.3.1. Pre-dried samples

472 From the TG and DTG curves shown in Figure 2, characteristic plots were
473 prepared for the model-free methods, i.e., Kissinger, Friedman, OFW, KAS, and
474 sDAEM. In the Kissinger plot, the logarithm of the heating rate β over the
475 temperature squared, T_{max}^2, for which the rate of reaction dα/dt is maximum
476 (Figure 2) is plotted as function of the inverse of this temperature, $1/T_{max}$, Eq. (3).
477 Since the maximum rate of reaction is attained at a specific temperature for each
478 heating rate, the Kissinger plot has only one data point for each heating rate.

479 According to the Friedman characteristic equation Eq. (4), the Friedman plot
480 shows the values of the logarithm of the rate of reaction dα/dt versus the inverse
481 temperature $1/T$. The OFW plot represents the logarithm of the heating rate β,

left-hand-side of the OFW characteristic equation Eq. (6), as a function of the inverse temperature $1/T$. Finally, KAS and sDAEM are based on similar characteristic equations Eq. (7) and Eq. (10), respectively, hence their plots coincide, depicting the logarithm of the heating rate β over temperature squared versus the inversed of temperature $1/T$ in both cases. The four different plots obtained from the pyrolysis measurements of beech wood conducted in the TG 209/2/F for the pre-dried samples are included in Figure 3. The plots derived from the measurements performed in the TGA Q500 are very similar to those shown in Figure 3, therefore, they are not included in the figure to avoid repetition.

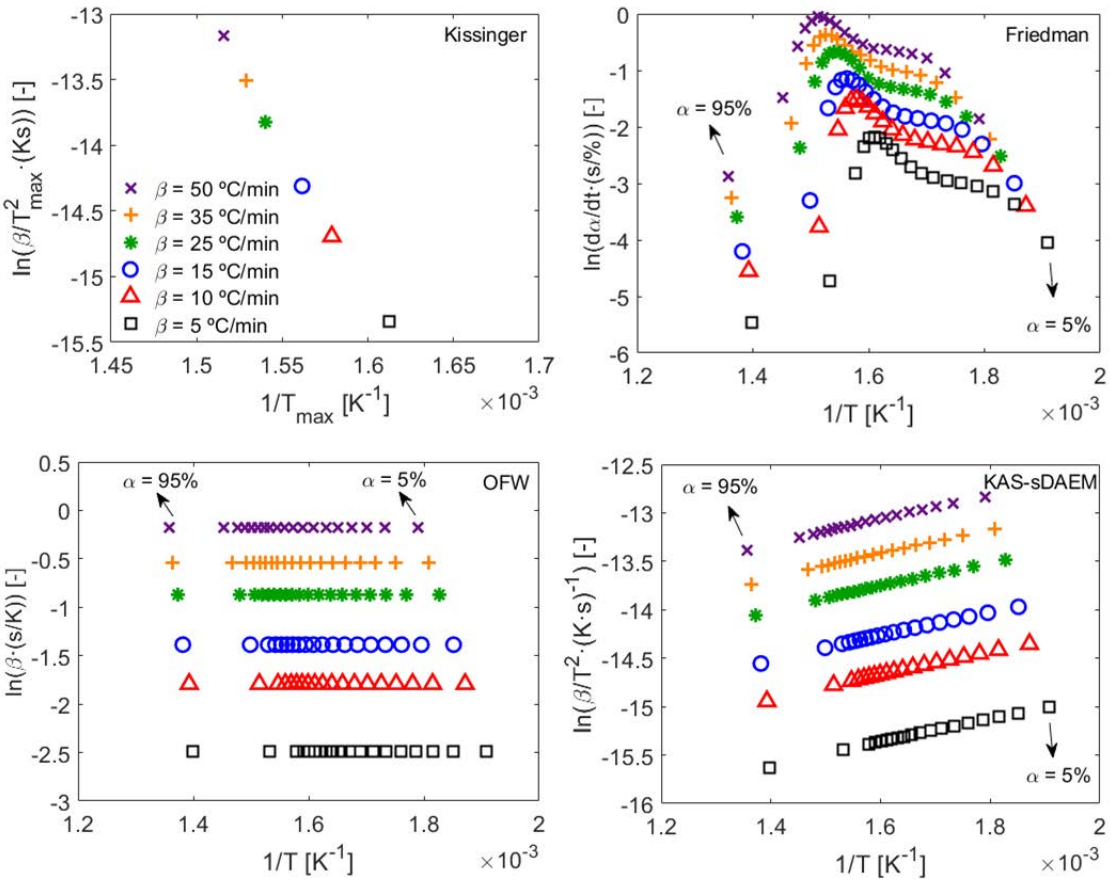

Figure 3: Data evaluation according to the different model-free kinetic methods applied to the pyrolysis measurements conducted in the TG 209/2/F (pre-dried samples).

The linearity of the data represented in the characteristic plots of Figure 3 is high, with coefficients of determination $R^2 \geq 0.995$ (Table 4), averaged in a degree of conversion range from 5% to 95%. The high R^2 values obtained from the pyrolysis measurements of pre-dried beech wood in both the TG 209/2/F and TGA Q500, reported in Table 4, reflect the high quality and reliability of the experimental measurements conducted in both instruments [9] and confirms the first-order assumption for the pyrolysis reactions.

Table 4: Coefficients of determination R^2 for the linear fitting of the characteristic plot data obtained from the pre-dried beech wood pyrolysis measurements in the TG 209/2/F and the TGA Q500.

	Kissinger	Friedman	OFW	KAS-DAEM
TG 209/2/F	0.998	0.997	0.999	0.995
TGA Q500	0.995	0.998	0.996	0.998

From the slope and intercept of the linear fits to the data in the characteristic plots, the pre-exponential factor *A* and activation energy *E* can be derived according to the characteristic equations. The values of the pre-exponential factors *A* and the activation energies *E* are shown in Figure 4 for a range of degree of conversion from 5 % to 95 %. The results from the two thermogravimetric analyzers are very similar. The conversion dependent values of *A* and *E* obtained from both the isoconversional methods and sDAEM show a similar behavior, with a roughly uniform value for a wide range of pyrolysis conversions from 5 % to around 85 %. Towards higher degrees of conversion, the values for *A* and *E* increase suddenly. This corresponds to the final slowdown of the conversion rate as seen in Figure 2. Hence, this is probably due to a dominance of the final char conversion processes.

As is obvious from Figure 4, the kinetic parameters obtained in the two instruments, by sDAEM and the isoconversional kinetic methods (KAS, OFW and Friedman) resulted in very similar values of *ln A* and *E*, differing by only 5-6 %. In contrast, Kissinger's method gave notably different values for *ln A* and *E* in the two instruments, differing by more than 20 %. Such deviations can be attributed to the simplicity of this data evaluation method and its differential character, which is liable to overrate the instrument noise, resulting in a reduction of the accuracy of the data evaluation [31]. The results of the kinetic parameters of beech wood pyrolysis derived in this work, shown in Figure 4, are in good agreement with those reported previously by Branca et al. [44], Ding et al. [62], Grønli et al. [63], and Di Blasi and Branca [64].

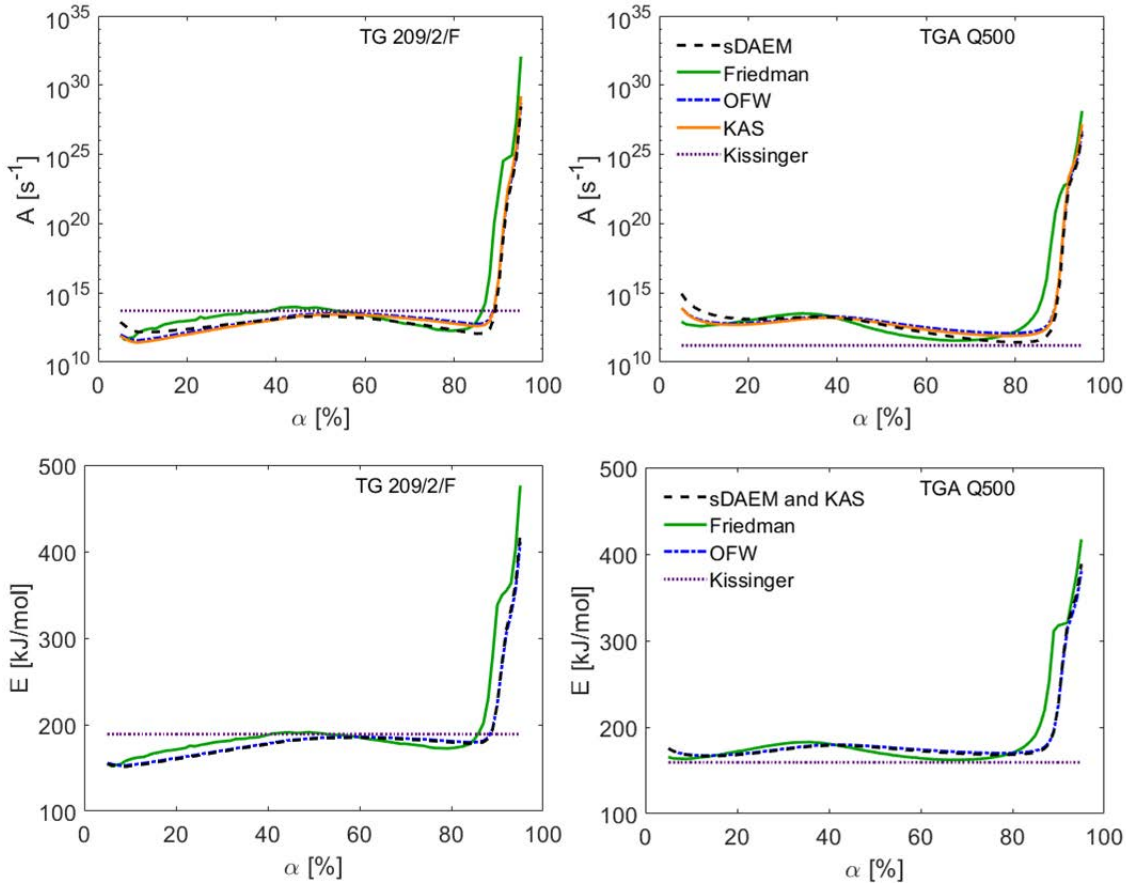

Figure 4: Kinetic parameters obtained from the various model-free kinetic methods applied to the pyrolysis measurements of pre-dried beech wood conducted in the TG 209/2/F and TGA Q500.

4.3.2. In situ dried samples

The results obtained from the pyrolysis of the in situ dried samples performed in the TGA Q500 were postprocessed similarly to the results of the pre-dried samples, using the same temperature range to determine the conversion degree, i.e., from 150 to 600 ºC, and applying the sDAEM to derive the kinetic parameters of the pyrolysis. The variations of the pre-exponential factor *A* and the activation energy *E* with the pyrolysis conversion degree α are shown in Figure 5 for the in situ and pre-dried tests carried out in the TGA Q500. The values of the kinetic parameters for the pre-dried and in situ dried samples are similar, obtaining average deviations of 3.2 % for *ln A* and 5.3 % for *E* over a range of the conversion degree from 5% to 85 %. However, a higher difference is obtained for high values of the conversion degree, corresponding to the pyrolysis of char, for which the kinetic parameters obtained applying sDAEM to the in situ dried samples are lower than those derived from the pre-dried samples. In view of the effect of humidity on the kinetic parameters of pyrolysis, drying the samples prior to the TGA pyrolysis tests (pre-drying) is recommended. However, if the sample must be dried in the TGA (in situ drying), the drying and pyrolysis processes should be properly separated by using a two-stage heating for the TGA pyrolysis tests to prevent any effect of humidity of the pyrolysis reactions.

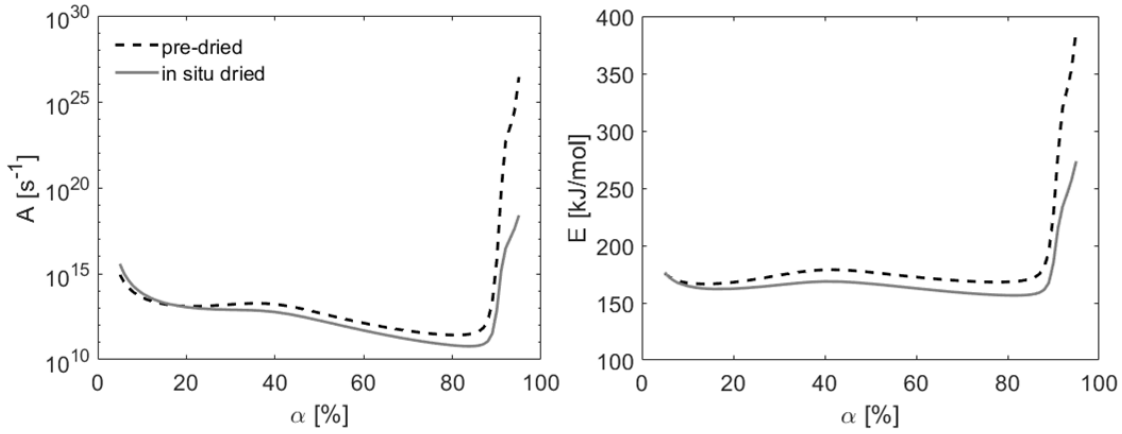

552

553 Figure 5: Kinetic parameters obtained applying sDAEM to the pyrolysis
554 measurements of pre-dried and in situ dried beech wood samples in the TGA
555 Q500.

556 4.4. Results of the five-step model

557 Figure 6 shows Kissinger plots of the experimental data for the pre-dried and the
558 in situ dried samples and compares them to the Kissinger plot that results from
559 the five-step model. For the pre-dried samples, the experimental data obtained
560 from the TG 209/2/F and TGA Q500 are in good agreement. However, if in situ
561 drying is applied, the temperatures of maximum decomposition rate, T_{max},
562 systematically decrease by around 15 K and the obtained kinetic parameters are
563 in closer agreement with the five-step model results. Perhaps, pre-drying and in
564 situ drying result in different surface properties and/or in different pore structures,
565 which lead to some change in the pyrolysis rate and/or reactions.

566 The resulting kinetic parameters are tabulated in Table 5. While all activation
567 energies are similar and are in the range E = 170 ± 15 kJ/mol for all cases, the
568 ordinate intercepts are quite different. In fact, the pre-exponential factors differ by
569 more than two orders of magnitude, giving $A = 10^{12.14 \pm 1.14}$ s^{-1}. Note, however, that
570 such a comparison has limitations, because it is based on the simplification of

571 Kissinger's method and because only one temperature is considered. A better
572 unifying view is presented in section 4.6 below.

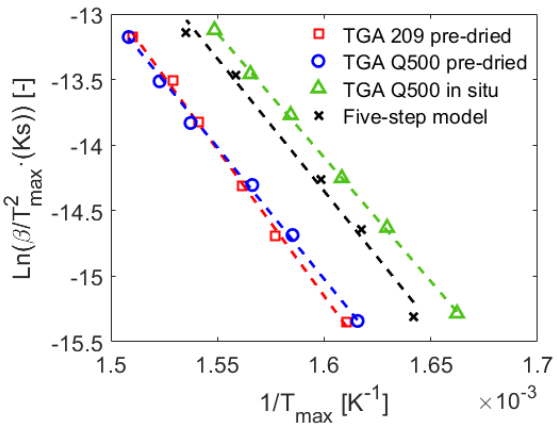

573

574 Figure 6: Kissinger plots of experimental data and five-step model.

575 Table 5: Comparison of overall kinetic data obtained from experiments and the
576 five-step model (Kissinger's method applied to both experimental and calculated
577 data).

Data set	A [s^{-1}]	E [kJ/mol]
TG 209/2/F, pre-dried	$1.9 \cdot 10^{13}$	185.4
TGA Q500, pre-dried	$5.3 \cdot 10^{11}$	166.9
TGA Q500, in situ dried	$2.0 \cdot 10^{11}$	157.2
Five-step model (TG 209/2/F)	$1.3 \cdot 10^{12}$	168.0

578

579 4.5. Effect of the final temperature selected for the pyrolysis process

580 The calculation of the degree of conversion by Eq. (14) is based on the selection
581 of appropriate initial and final temperatures for the pyrolysis process. The
582 selection of these temperatures may affect the results obtained for the kinetic
583 parameters of the pyrolysis reaction, because (i) in the initial stage, up to about
584 120 °C, the mass loss is due to the drying process, (ii) in the final stage, above

585 about 400 °C, the mass loss is mainly due to the thermal decomposition of the
586 residual char.

587 Only in between these temperatures, the mass loss is really dominated by the
588 release of original volatile matter. Therefore, the initial temperature should be
589 selected as a value higher than the drying temperature, i.e., around 100 ºC for
590 atmospheric processes, and below the minimum temperature for the onset of the
591 release of volatiles. The value selected for the initial temperature has only little
592 effect on the kinetic results provided that the degree of pyrolysis conversion below
593 this value is negligible. A typical value is 150 ºC, since the devolatilization of
594 biomass occurs at temperatures above this value. In contrast, the proper choice
595 of the end point of the pyrolysis process is not so easy to define *a priori*.

596 Figure 7 a) shows the evolution with temperature of the percentage of mass
597 remaining in the TGA Q500, *X*, during the pyrolysis of beech wood at a heating
598 rate of 5 ºC/min. The slope of the curve of mass percentage versus temperature
599 is negligible for a temperature around 150 ºC, thus, this is a proper value for the
600 initial temperature of the pyrolysis process. Furthermore, the selection of a
601 different value for the initial temperature has no effect on the kinetic parameters
602 obtained, provided that it is selected in the plateau zone of the TG curve after the
603 drying process.

604 As indicated above, the selection of the final temperature of the pyrolysis process
605 is more complex since, after the steep reduction of the mass percentage due to
606 the release of the volatile matter of the sample (at around 300 ºC in Figure 7 a)),
607 the mass percentage continues to decrease at a lower rate because of the
608 reduced amount of volatiles and because of the onset of the slow thermal

609 degradation of char (for temperatures above 400 ºC in Figure 7 a)). Unfortunately,
610 the pyrolysis conversion rate does not become zero at high temperatures after
611 the consumption of the volatile matter, due to the continuing slow decomposition
612 of the remaining char. Therefore, the selection of the final temperature of
613 pyrolysis is somewhat arbitrary and may affect the results obtained for the
614 activation energy and the pre-exponential factor of the total mass loss during the
615 pyrolysis process. To quantify this effect, a sensitivity analysis of the value of this
616 final temperature on the values obtained from sDAEM for the kinetic parameters
617 of pyrolysis was carried out. Four values of the final temperature of the pyrolysis
618 process of 450, 600, 750, and 900 ºC were chosen. The degree of conversion
619 during pyrolysis as a function of temperature for the various final temperatures
620 studied can be seen in Figure 7 b). The evolution of the pyrolysis conversion
621 degree with temperature is quite similar in all cases for values of the degree of
622 conversion below 80 %, i.e., for temperatures below 400 ºC, in what is called the
623 active stage of pyrolysis, where pyrolysis of hemicellulose and cellulose, and
624 partly lignin, occurs. However, for higher values of the degree of conversion, i.e.,
625 for temperatures between 400 and 900 ºC, the passive stage of pyrolysis takes
626 place, which is dominated by the pyrolysis of the lignin contained in char [63,64].
627 Significant differences are observed for the evolution of the conversion at
628 temperatures above 400 ºC, depending on the final temperature selected for the
629 pyrolysis process. The differences occurring for these high temperatures are
630 caused by the increasing importance of devolatilization of lignin contained in char
631 at higher temperatures.

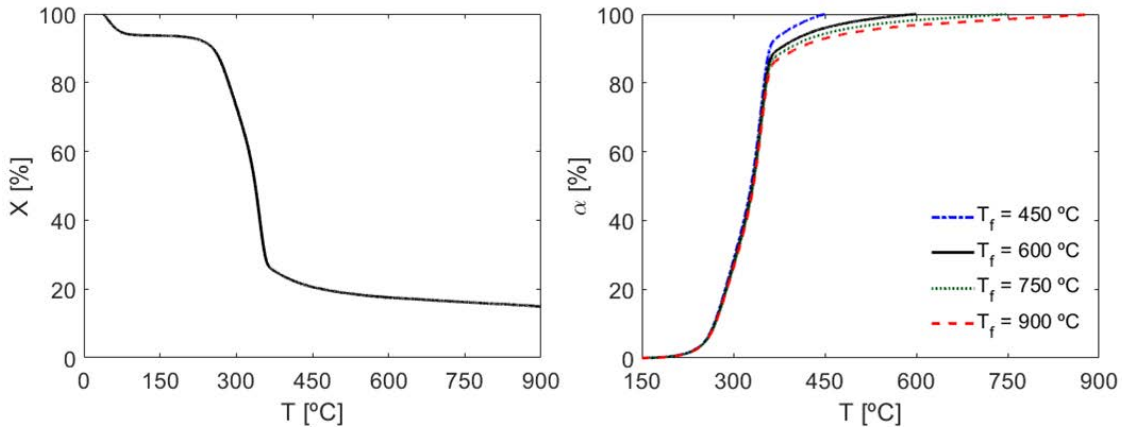

Figure 7: a) Evolution of the percentage of mass remaining with temperature during the pyrolysis of beech wood in the TGA Q500 at 5 ºC/min (pre-dried sample), b) Evolution of the degree of conversion with temperature during the pyrolysis of beech wood in the TGA Q500 at 5 ºC/min for various final temperatures (pre-dried sample).

Considering the curves of the pyrolysis conversion degree versus temperature depicted in Figure 7 b) for the various final temperatures analyzed, the sDAEM was applied to determine the kinetic parameters of beech wood pyrolysis, i.e., the activation energy and pre-exponential factor, as a function of the degree of conversion for each final temperature selected. The results of the kinetic parameters as a function of the conversion degree are shown in Figure 8. They show similar values for the kinetic parameters derived for α below 80 %. In contrast, for degrees of conversion above 80 %, both the pre-exponential factor and the activation energy increase substantially when the final temperature selected for the pyrolysis process is higher. These differences are caused by the increasing importance of char pyrolysis towards higher final temperatures. For instance, if the final temperature is chosen to be 450 °C, a degree of conversion of 90 % corresponds closely to the end of the release of biomass volatile matter

(see Figure 7 a)). However, if the final temperature is chosen to be 900 °C, the same degree of conversion corresponds to the ongoing thermal degradation of the char produced, and of course, these completely different chemical reactions have different kinetic parameters associated. Therefore, the final temperature selected for the pyrolysis process influences the kinetic parameters obtained for high degrees of conversion. It is recommended to select a final temperature up to which the derivative of the mass percentage remaining, *X*, has a low value and starts to decrease steadily. In the present study of beech wood pyrolysis, it was found most appropriate to select a final temperature of 600 °C for the evaluation of the kinetic data.

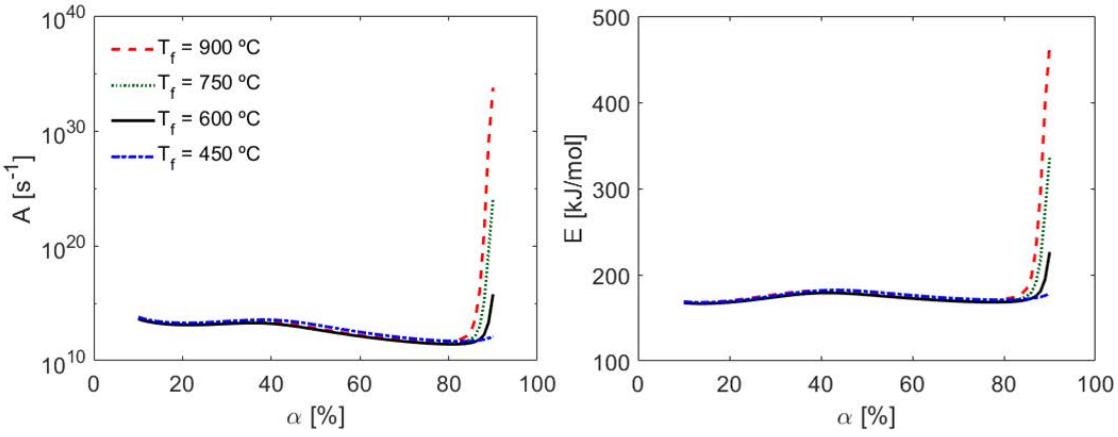

Figure 8: Kinetic parameters obtained from the sDAEM for the pyrolysis measurements of beech wood conducted in the TGA Q500 considering various final temperatures for the pyrolysis process (pre-dried samples).

4.6. Discussion on the capabilities of model-free and model-fitting kinetic methods

As noticed in sections 1 and 2, the values of kinetic parameters derived from TG investigations may show notable differences. These are somewhat difficult to interpret due to the non-linear character of the reaction kinetics. The problem can

be solved by choosing a more unifying benchmark for the comparison. In that sense, TG or DTG curves can be reconstructed from the fitted kinetic data which directly illustrate the data quality by comparison to the experimental measurements.

As example, the experiment with a pre-dried sample, pyrolyzed at a heating rate of 25 ºC/min in the TGA Q500, was chosen. The TG curves were recalculated using the kinetic parameters as derived from the sDAEM, integral isoconversional methods of OFW and KAS, Friedman and Kissinger methods, as well as by the five-step model. The recalculated curves of Friedman, OFW, and KAS were obtained by solving their characteristic equations, i.e., Eqs. (4), (6), and (7), respectively, whereas Eq. (10) was solved to obtain the recalculated curve of sDAEM. In contrast, the recalculated curves of the Kissinger method and the five-step fitting model were derived by integration of $dm/dt = - k \cdot m$, considering the kinetic parameter to determine the rate coefficient, Eq. (2). The results are shown in Figure 9 and compared to the experimental TG curve. The sDAEM, KAS and OFW methods reproduce the experimental data with high accuracy. The deviations from the measured degree of conversion are less than 0.15 %, hence the three results collapse on a single curve in Figure 9. The other methods give less accurate results in the order Friedman's method > five-step model > Kissinger's method. An extra pyrolysis experiment was conducted at 75 ºC/min, a higher heating rate than those use to derive the kinetic parameters, to check the capability of the kinetic methods to predict TG curves at higher heating rates. The results obtained, also depicted in Figure 9, are similar to those at 25 ºC/min, with a slight shift to higher temperatures of the conversion estimation of the five-step model.

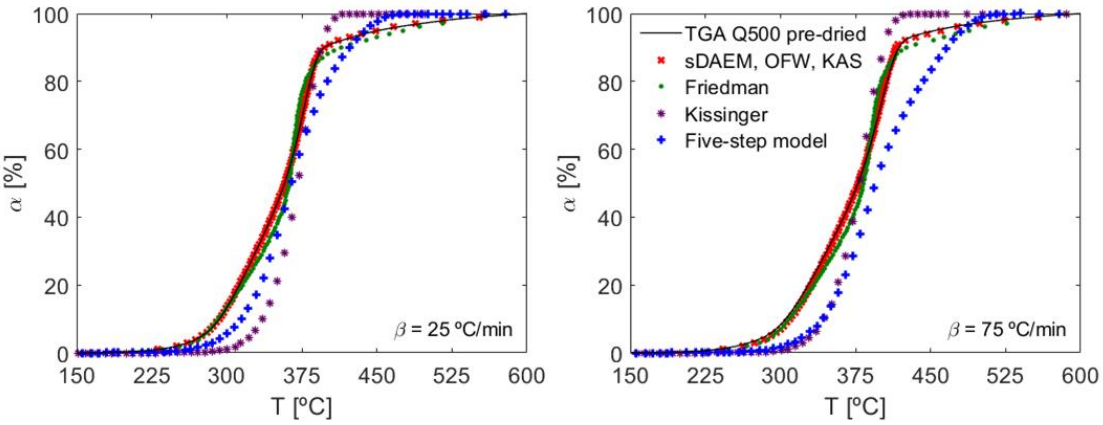

Figure 9: Comparison of the TG curve measured in the TGA Q500 for the pre-dried sample and the recalculated curves obtained by the kinetic models at 25 °C/min and 75 °C.

As noticed before, Friedman's model suffers from the differential character of the method and Kissinger's method appears to be an oversimplification in case of mixtures of substances and polymers. Regarding the five-step model, some disagreement with the experimental TG curve was expected according to Figure 6. However, the five-step model also allows an estimate of the pyrolysis gas composition, which is not a subject in this work.

Among the model-free methods, the integral methods OFW, KAS and sDAEM are found to be superior to the differential method of Friedman or the simple Kissinger method. Regarding model-fitting methods, they clearly have the advantage to allow predictions of the pyrolysis gas composition, in contrast, they often appear to have problems to reproduce the final, slow pyrolysis of char correctly. It appears that for wood pyrolysis, there is no direct comparison of several model-fitting methods available in the literature.

5. Conclusions

713 The kinetics of beech wood pyrolysis was studied by means of non-isothermal
714 thermogravimetric measurements conducted in two different thermogravimetric
715 analyzers (TGA), a TG 209/2/F from Netzsch and a TGA Q500 from TA
716 Instruments. Both instruments were found to have a high repeatability and
717 accuracy for the temperature control. Model-free methods, isoconversional
718 models, the simplified distributed activation energy model (sDAEM), and a model-
719 fitting method, the five-step model, were used to determine the kinetic parameters
720 of the pyrolysis reactions. Except for Kissinger's method, the kinetic parameters,
721 obtained from the experimental results in both analyzers were in very good
722 agreement. The kinetic data obtained from the different evaluation methods were
723 compared by reconstruction of the thermogravimetric curves. In this way, the
724 performance of methods of Ozawa, Flynn and Wall (OFW), Kissinger-Akahira-
725 Sunose (KAS) and sDAEM were found to be excellent. Friedman's method,
726 Kissinger's method and the five-step model gave somewhat less good results,
727 partly due to the corresponding mathematical procedure and partly due to the
728 adopted simplifications. Hence, from the point of view of accurate data
729 approximation, the integral isoconversional methods and sDAEM are
730 recommended. From the point of view of detailed mechanistic information and
731 product formation, model-fitting methods are required, probably increasing the
732 accuracy with an increasing number of reactions, with sDAEM representing the
733 limiting case of an infinite set of reaction steps.

734 In addition, the pyrolysis process was analyzed for pre-dried beech wood
735 samples and for in situ dried samples, i.e., for a sample dried in the TGA as an
736 immediate process prior to the pyrolysis. The in situ dried sample was found to
737 pyrolyze faster than the pre-dried sample, and the experimental pyrolysis rates

738 were close to those of the five-step model. The effect of the final temperature
739 selected for the pyrolysis process was also analyzed, finding that both the pre-
740 exponential factor and the activation energy increased significantly for higher
741 values of the final pyrolysis temperature, as a consequence of the greater
742 importance of the slow thermal degradation of char at elevated temperatures.

743 **Acknowledgments**

744 The authors express their gratitude to the BIOLAB experimental facility, to the
745 “Programa de movilidad de investigadores en centros de investigación
746 extranjeros (Modalidad A)” from the Carlos III University of Madrid (Spain) and to
747 the Institute of Combustion Technology at DLR for the financial support conceded
748 to Antonio Soria-Verdugo for a research stay at the German Aerospace Center
749 DLR (Stuttgart, Germany) during the summer of 2018.

750 Funding by the Helmholtz Association of German Research Centers in the
751 research fields energy, fuels and gasification, especially in the Program “Energy
752 Efficiency, Materials and Resources“, is acknowledged by the Institute for
753 Technical Chemistry at KIT, Karlsruhe, and by the Institute of Combustion
754 Technology at DLR Stuttgart.

755 **References**

756 [1] Asadullah M. Barriers of commercial power generation using biomass
757 gasification gas: a review. Renew Sustain Energy Rev 2014; 29, 201-215.

758 [2] McKendry P. Energy production from biomass (part 2): conversion
759 technologies. Bioresour. Technol. 2002; 83, 47-54.

760 [3] Basu P. Biomass gasification and pyrolysis - Practical design and theory.
761 Elsevier Inc.; 2010.

762 [4] Dhyani V., Bhaskar T. A comprehensive review on the pyrolysis of
763 lignocellulosic biomass. Renew Energy 2018; 129, 695-716.

764 [5] Papadikis K., Gu S., Bridgwater A.V., Gerhauser H. Application of CFD to
765 model fast pyrolysis of biomass. Fuel Process. Technol. 2009; 90, 504-512.

766 [6] Wang S., Dai G., Yang H., Luo Z. Lignocellulosic biomass pyrolysis
767 mechanism: a state-of-the-art review. Prog. Energy Combust. Sci. 2017; 62, 33-
768 86.

769 [7] Vyazovkin S., Burnham A.K., Criado J.M., Pérez-Maqueda L.A., Popescu C.,
770 Sbirrazzuoli N. ICTAC kinetics committee recommendations for performing
771 kinetic computations on thermal analysis data. Thermochim. Acta 2011; 520, 1-
772 19.

773 [8] Cai J., Wu W., Liu R. An overview of distributed activation energy model and
774 its application in the pyrolysis of lignocellulosic biomass. Renew. Sust. Energ.
775 Rev. 2014; 36, 236-246.

776 [9] Anca-Couce A. Reaction mechanisms and multi-scale modelling of
777 lignocellulosic biomass pyrolysis. Prog. Energy Combust. Sci. 2016; 53, 41-79.

778 [10] Soria-Verdugo A., Goos E., García-Hernando N., Riedel U. Analyzing the
779 pyrolysis kinetics of several microalgae species by various differential and
780 integral isoconversional kinetic methods and the Distributed Activation Energy
781 Model. Algal Res. 2018a; 32, 11-29.

782 [11] Arrhenius S. Über die Reaktionsgeschwindigkeit bei der Inversion von
783 Rohrzucker durch Säuren (On the reaction velocity of the inversion cane sugar
784 by acids). Z. Phys. Chem. 1889; 4, 226-248.

785 [12] Hemminger W.F., Cammenga H.K. Methoden der thermischen Analyse.
786 Berlin, Germany, Springer, 1989.

787 [13] Khawam A., Flanagan D.R. Basics and Applications of Solid-State Kinetics:
788 A Pharmaceutical Perspective. J. Pharm. Sci. 2006; 95, 472-498.

789 [14] Pérez-Maqueda L.A., Sánchez-Jiménez P.E., Criado J.M. Kinetic Analysis
790 of Solid-State Reactions: Precision of the Activation Energy Calculated by
791 Integral Methods. Int. J. Chem. Kinet. 2005; 37, 658–666.

792 [15] Broido A., Weinstein M. Kinetics of solid-phase cellulose pyrolysis. In:
793 Wiedemann, ed., Proceedings of the 3rd International Conference on Thermal
794 Analysis. 1971, p. 285-296, Basel, Birkhauser Verlag.

795 [16] Shafizadeh F. Introduction to pyrolysis of biomass. J. Anal. Appl. Pyrol. 1982;
796 3, 283-305.

797 [17] Antal M.J.; Várhegyi G. Impact of Systematic Errors on the Determination of
798 Cellulose Pyrolysis Kinetics. Energy Fuels 1997; 11, 1309-1310.

799 [18] Conesa J.A., Caballero, J.A., Marcilla, A., Font, R. Analysis of different kinetic
800 models in the dynamic pyrolysis of cellulose. Thermochim. Acta 1995; 254, 175-
801 192.

802 [19] Lin T., Goos E., Riedel U., A sectional approach for biomass: Modelling the
803 pyrolysis of cellulose. Fuel Processing Technology 2013; 115, 246-253.

804 [20] Grønli M., Antal M.J., Várhegyi G. A round-robin study of cellulose pyrolysis
805 kinetics by thermogravimetry. Ind. Eng. Chem. Res. 1999; 38, 2238-2344.

806 [21] Maciejewski M. Computational aspects of kinetic analysis. Part B: The ICTAC
807 Kinetics Project - the decomposition kinetics of calcium carbonate revisited, or
808 some tips on survival in the kinetic mine field. Thermochim. Acta 2000; 355, 145-
809 154.

810 [22] Antal M.J., Várhegyi G., Jakab E. Cellulose pyrolysis kinetics: Revisited. Ind.
811 Eng. Chem Res.1998; 37, 1267-1275.

812 [23] Anca-Couce A., Berger A., Zobel N. How to determine consistent biomass
813 pyrolysis kinetics in a parallel reaction scheme. Fuel 2014; 123, 230-240.

814 [24] Kissinger H.E. Variation of peak temperature with heating rate in differential
815 thermal analysis. J. Res. Natl. Bur. Stand. 1956; 57, 217-221.

816 [25] Kissinger H.E., Reaction kinetics in differential thermal analysis. Anal. Chem.
817 1957; 29, 1702-1706.

818 [26] Vyazovkin S. Isoconversional kinetics. In: Handbook of Thermal Analysis and
819 Calorimetry Vol.5: Recent Advances, Techniques and Applications. 2008,
820 Elsevier B.V. M.E. Brown and P.K. Gallagher (Editors), Chapter 13, pages 503-
821 538.

822 [27] Friedman H. L. Kinetics of thermal degradation of char-forming plastics from
823 thermogravimetry. Application to a phenolic plastic. J. Polym. Sci. C. 1964; 6,
824 183-195.

825 [28] Ozawa T. A new method of analyzing thermogravimetric data. Bull. Chem.
826 Soc. Jpn. 1965; 38, 1881-1886.

827 [29] Flynn J. H., Wall L. A. General treatment of the thermogravimetry of
828 polymers. J. Res. Nat. Bur. Standards. 1966; 70A, 487-523.

829 [30] Akahira T., Sunose T. Method of determining activation deterioration
830 constant of electrical insulating materials. Res. Rep. Chiba Inst. Technol. 1971;
831 16, 22-31.

832 [31] Vyazovkin S. Evaluation of activation energy of thermally stimulated solid-
833 state reactions under arbitrary variation of temperature. J. Comput. Chem. 1997;
834 18, 393-402.

835 [32] Doyle C.D. Estimating isothermal life from thermogravimetric data. J. Appl.
836 Polym. Sci. 1962; 6, 639-642.

837 [33] P. Murray, J. White. Kinetics of the thermal dehydration of clays. IV.
838 Interpretation of the differential thermal analysis of the clay minerals. Trans. Brit.
839 Ceram. Soc. 1955; 54, 204-238.

840 [34] M.J. Starink. The determination of activation energy from linear heating rate
841 experiments: a comparison of the accuracy of isoconversion methods.
842 Thermochim. Acta 2003; 404, 163-176.

843 [35] Vand V. A theory of the irreversible electrical resistance changes of metallic
844 films evaporated in vacuum. Proc. Phys. Soc. 1943; 55, 222-246.

845 [36] Miura K. A new and simple method to estimate f(E) and k_0(E) in the
846 distributed activation energy model from three sets of experimental data. Energ.
847 Fuel 1995; 9, 302-307.

848 [37] Miura K., Maki T. A simple method for estimating f(E) and k_0(E) in the
849 distributed activation energy model. Energ. Fuel 1998; 12, 864-869.

850 [38] Coats A.W., Redfern J.P. Kinetic parameters from thermogravimetric data.
851 Nature. 1964; 201, 68-69.

852 [39] Soria-Verdugo A., Goos E., García-Hernando N. Effect of the number of TGA
853 curves employed on the biomass pyrolysis kinetics results obtained using the
854 Distributed Activation Energy Model. Fuel Process. Technol. 2015; 134, 360-371.

855 [40] Soria-Verdugo A., Goos E., Morato-Godino A., García-Hernando N., Riedel
856 U. Pyrolysis of biofuels of the future: Sewage sludge and microalgae -
857 Thermogravimetric analysis and modelling of the pyrolysis under different
858 temperature conditions. Energ. Convers. Manage. 2017; 138, 261-272.

859 [41] Soria-Verdugo A., Goos E., Arrieta-Sanagustín J., García-Hernando N.
860 Modeling of the pyrolysis of biomass under parabolic and exponential
861 temperature increases using the Distributed Activation Energy Model. Energ.
862 Convers. Manage. 2016; 118, 223-230.

863 [42] Soria-Verdugo A., Rubio-Rubio M., Goos E., Riedel U. Combining the
864 lumped capacitance method and the simplified distributed activation energy
865 model to describe the pyrolysis of thermally small biomass particles. Energ.
866 Convers. Manage. 2018b; 175, 164-172.

867 [43] Couhert C., Commandre J.M., Salvador S. Is it possible to predict gas yields
868 of any biomass after rapid pyrolysis at high temperature from its composition in
869 cellulose, hemicellulose and lignin? Fuel 2009; 88, 408-417.

870 [44] Branca C., Albano A., Di Blasi C. Critical evaluation of global mechanisms of
871 wood devolatilization. Thermochim. Acta 2005; 429, 133-141.

872 [45] Mätzing H., Gehrmann H.J., Merz D., Kolb T., Seifert H. A five step pyrolysis
873 mechanism for wood burning models. Proceedings of the 19th European
874 Biomass Conference. Berlin, Germany. Florence, Italy: ETA-Florence Renewable
875 Energies, 2011. http://www.etaflorence.it/proceedings/register.asp

876 [46] Schinkel A.P. Zur Modellierung der Biomassepyrolyse im Drehrohrreaktor,.
877 Ph.D. Thesis, Universität Kassel, Germany, 2002.

878 [47] Di Blasi C. Modeling chemical and physical processes of wood and biomass
879 pyrolysis. Prog. Energy Comb. Sci. 2008; 34, 47–90.

880 [48] Ranzi E., Cuoci A., Faravelli T., Frassoldati A., Migliavacca G., Pierucci S.,
881 Sommariva S. Chemical kinetics of biomass pyrolysis. Energy Fuels 2008; 22,
882 4292–4300.

883 [49] Tomasi Morgano M., Leibold H., Richter F., Seifert H. Screw pyrolysis with
884 integrated sequential hot gas filtration. J. Anal. Appl. Pyrol. 2015; 113, 216-224.

885 [50] Mätzing H., Gehrmann H.J., Seifert H., Stapf D. Modelling grate combustion
886 of biomass and low rank fuels with CFD application. Waste Manage 2018; 78,
887 686-697.

888 [51] Mätzing H., Baris D., Ciuta S., LeBlanc J., Castaldi M.J., Gehrmann H.J.,
889 Stapf D. A comparison of wood pyrolysis products obtained by thermogravimetry
890 and intra-particle measurements. 6th International Conference on Engineering
891 for Waste and Biomass Valorisation (WasteEng 2016), Albi, France, 2016 p. 510-
892 517.

893 [52] Tomasi Morgano M. Screw pyrolysis of biogenic feedstock with integrated
894 hot gas filtration. PhD thesis, University of Stuttgart, 2019.

895 [53] Beuth; 2019. https://www.beuth.de/de/regelwerke,
896 https://europa.eu/european-union/business/eu-standards_de

897 [54] Klemm D., Philipp B., Heinze T., Heinze U., Wagenknecht W.
898 Comprehensive Cellulose Chemistry: Fundamentals and Analytical Methods,
899 Volume 1. Wiley, 1998.

900 [55] Vyazovkin S., Chrissafis K., di Lorenzo M.L., Koga N., Pijolat M., Roduit B.,
901 Sbirrazzuoli N., Suñol J.J. ICTAC Kinetics Committee recommendations for
902 collecting experimental thermal analysis data for kinetic computations.
903 Thermochim. Acta, 2014; 590, 1-23.

904 [56] Soria-Verdugo A., García-Hernando N., Garcia-Gutierrez L.M., Ruiz-Rivas
905 U. Analysis of biomass and sewage sludge devolatilization using the distributed
906 activation energy model. Energ. Convers. Manage. 2013; 65, 239-244.

907 [57] Soria-Verdugo A., Garcia-Gutierrez L.M., Blanco-Cano L., Garcia-Hernando
908 N., Ruiz-Rivas U. Evaluating the accuracy of the Distributed Activation Energy
909 Model for biomass devolatilization curves obtained at high heating rates. Energ.
910 Convers. Manage. 2014; 86, 1045-1049.

911 [58] Lei Q., Xie Q., Ding Y. Fire hazard evaluation of activated carbons. J. Therm.
912 Anal. Calorim. 2020; 139, 441-449.

913 [59] Radhakrishnan K., Hindmarsh, A. Description and use of LSODE, the
914 Livermore solver for ordinary differential equations, Technical report UCRL-ID-
915 113855, Lawrence Livermore National Laboratory, 1993.

916 [60] Munir S., Daood S.S., Nimmo W., Cunliffe A.M., Gibbs B.M. Thermal analysis
917 and devolatilization kinetics of cotton stalk, sugar cane bagasse and shea meal
918 under nitrogen and air atmospheres. Bioresour. Technol. 2009; 100, 1413-1418.

919 [61] Tonbul Y., Saydut A., Yurdakoc K., Hamamci C. A kinetic investigation on
920 the pyrolysis of Seguruk asphaltite. J. Therm. Anal. Calorim. 2009; 95, 197-202.

921 [62] Ding Y., Ezekoye O.A., Lu S., Wang C. Thermal degradation of beech wood
922 with thermogravimetry/Fourier transform infrared analysis. Energ. Convers.
923 Manage. 2016; 120, 370-377.

924 [63] Grønli M.G., Várhegyi G., Di Blasi C. Thermogravimetric analysis and
925 devolatilization kinetics of wood. Ind. Eng. Chem. Res. 2002; 41, 4201-4208.

926 [64] Di Blasi C., Branca C. Kinetics of primary formation from wood pyrolysis. Ind.
927 Eng. Chem. Res. 2001; 40, 5547-5556.

928 [65] K.G. Mansaray, A.E. Ghaly. Thermal degradation of rice husks in nitrogen
929 atmosphere. Bioresour. Technol. 1998; 65, 13-20.

930 [66] K. Slopiecka, P. Bartocci, F. Fantozzi. Thermogravimetric analysis and
931 kinetic study of poplar wood pyrolysis. Appl. Energ. 2012; 97, 491-497.

List of figures

952 Figure 9: Comparison of the TG curve measured in the TGA Q500 for the pre-
953 dried sample and the recalculated curves obtained by the kinetic models at 25
954 ºC/min and 75 ºC.

List of tables